Mechanically induced structural changes during dynamic compression of engineered cartilaginous constructs can potentially explain increases in bulk mechanical properties

Thomas Nagel and Daniel J. Kelly[1]

Trinity Centre for Bioengineering, Dept. of Mechanical and Manufacturing Engineering, Trinity College Dublin, Dublin 2, Ireland

Summary Several studies on chondrocyte seeded hydrogels in bioreactor culture report increased mechanical properties of mechanically loaded constructs compared to unloaded free swelling controls despite no significant differences in biochemical composition. One possible explanation is that changes in the collagen architecture of dynamically compressed constructs lead to improved mechanical properties. Collagen molecules are incorporated locally into the extracellular matrix with individual stress-free configurations and orientations. In this study we isolated and computationally investigated possible influences of loading on the collagen architecture in chondrocyte seeded hydrogels and their resulting mechanical properties. Both the collagen orientation and its stress-free configuration were hypothesised to depend on the local mechanical environment. Reorientation of the collagen network alone in response to dynamic compression leads to a prediction of constructs with lower compressive properties. In contrast, remodelling of stress-free configurations of collagen fibres was predicted to result in compacted tissues with higher swelling pressures and an altered pre-stressed state of the collagen network. Combining both mechanisms resulted in predictions of construct geometry and mechanical properties in agreement with experimental observations. This study provides support for the hypothesis that structural changes to the collagen network contribute to the enhanced mechanical properties of cartilaginous tissues engineered in bioreactor culture.

Key terms: mechanobiology; collagen remodelling; natural configuration; bioreactor; chondrocytes

1 Introduction

The aim of functional tissue engineering is to create viable substitutes to repair damaged tissues. Many tissue engineering strategies rely on some form of scaffold or hydrogel that is seeded with and infiltrated by cells. The cells then synthesise phenotype-specific extracellular matrix (ECM), ideally generating a mechanically functional tissue. The specific biomolecules synthesised by the cells and incorporated into the ECM make up the tissue composition which in turn dictates the basic biomechanical properties of the tissue. The relationships between tissue composition and mechanical function have been the subject of many studies on articular cartilage (e.g. [1, 2, 3]).

[1]kellyd9@tcd.ie

Besides the biochemical composition another key determinant of biomechanical performance is the structural arrangement of the various constituents and their interactions. Connective tissues usually have a very distinct collagen architecture: Articular cartilage exhibits a typical zonal variation in its collagen network ranging from parallel to the articular surface in the superficial zone to perpendicular in the deep zone [4]; collagen fibres in the menisci are predominantly oriented circumferentially leading to a transversely isotropic material with a very high circumferential stiffness [5]; other examples of soft tissues with a highly organised collagen structure include tendons, ligaments, periosteum and arteries.

Biological tissues adapt their structure to their mechanical environment [6]. A collagen architecture responsive to the mechanical environment has been observed and computational models have been used to study this phenomenon in many tissues, including cardiovascular [7, 8, 9, 10, 11], articular cartilage [12, 13, 14, 15], tendon [16] and during skeletal tissue regeneration [17, 18]. In many of these studies the collagen network has been hypothesised to align with respect to the principal directions of local mechanical regulators. In addition to orientational remodelling the notion of natural configurations has been documented. Since proteins are incorporated into the extracellular matrix at different time points and different deformation states, they have individual stress-free configurations [19]. Due to ongoing synthesis, degradation and remodelling the tissue's stress-free configurations evolve. In the context of a collagen fibre, an implication of this is that the recruitment stretch, i.e. the stretch at which the fibre becomes uncrimped and begins to bear load, can evolve. Remodelling of this stress-free state plays a role in scaffold contraction [20] and tissue growth and remodelling [21, 22, 23, 24].

Articular cartilage has been in the focus of numerous tissue engineering studies [25, 26, 27, 28]. Many of these have shown increases in metabolic or synthetic cell activities due to dynamic loading in addition to enhanced mechanical properties [29, 30, 31, 32, 33]. Other studies on chondrocyte seeded hydrogels in bioreactor culture have found increased mechanical properties of mechanically loaded constructs compared to unloaded free swelling controls despite no significant differences in biochemical composition [34, 35, 36, 37]. Similar results have been observed for mesenchymal stem cells undergoing chondrogenesis while subjected to dynamic compression [38].

Enhanced structural organisation has been suggested as one possible explanation for these latter results in the experimental literature ([39, 40, 35, 37]). However, this has not been directly tested experimentally and its influence – both in nature and in magnitude – on the mechanical properties remains largely unknown. Dynamic loading causes biochemical, biomechanical, compositional and nutritional alterations that are all potential contributors to the observed changes. Unravelling the relative contribution of the involved mechanisms is complex and challenging. Computational models offer the advantage of allowing for systematic investigation of individual mechanisms without altering other aspects of the system, which is often not feasible experimentally. The hypothesis under investigation in this study is that changes in the local collagen orientation and/or stress-free configuration in response to loading can lead to enhanced bulk mechanical properties of tissue

engineered cartilaginous constructs due to mechanical loading in the absence of alterations to the biochemical composition, i.e. material parameters. To test this hypothesis, model predictions of changing construct geometry and mechanical properties due to structural changes in the collagen network in response to dynamic compression will be compared to the results of bioreactor studies where chondrocyte seeded agarose constructs are subjected to dynamic compression [35, 36]. Structural changes to the engineered tissues were studied using a previously developed remodelling framework [41]. This and similar frameworks have been successful in predicting changes in collagen fibre orientation and stress-free configuration in a large number of biological tissues and cell seeded hydrogel systems which suggests that the underlying principles are of general significance in load-bearing tissues.

2 Materials & Methods

2.1 Material Model

A large strain biphasic material model with osmotic swelling effects was used [42, 43]. The total stress $\boldsymbol{\sigma}$ in the biphasic medium is given as:

$$\boldsymbol{\sigma} = -(p + \Delta\pi)\boldsymbol{I} + \boldsymbol{\sigma}_E \tag{1}$$

Here, p is the hydraulic pore pressure, $\boldsymbol{\sigma}_E$ the solid extra Cauchy stress and $\Delta\pi$ the Donnan osmotic pressure inside the tissue given by

$$\Delta\pi = 2RT\left[\sqrt{c_{ext}^2 + \frac{(c_{F0}\phi_{F0})^2}{4(J-\phi_{S0})^2}} - c_{ext}\right] \tag{2}$$

where $R = 8.3145\,\frac{\mathrm{N\,mm}}{\mathrm{mmol\,K}}$ is the universal gas constant, c_{ext} the external salt concentration, T the absolute temperature, c_{F0} the initial fixed charge density and J the determinant of the deformation gradient $\boldsymbol{F}$. The initial porosity ϕ_{F0} and solidity ϕ_{S0} are linked via the saturation condition $\phi_{F0} + \phi_{S0} = 1$.

The solid extra stresses were derived from free Helmholtz energy density functions that were split into isotropic and anisotropic parts. For the isotropic part we used a Neo-Hookean formulation

$$\psi_{iso} = C_1(I_1 - \ln I_3 - 3) + D_2(\ln I_3)^2 \tag{3}$$

with the first and third principal invariant I_1 and I_3 of the right Cauchy-Green tensor $\boldsymbol{C} = \boldsymbol{F}^T\boldsymbol{F}$. To describe structural remodelling of the collagen network an evolving remodelled configuration was introduced via a multiplicative decomposition of the deformation gradient

$$\boldsymbol{F} = \boldsymbol{F}_e\boldsymbol{F}_r \tag{4}$$

The part of the deformation denoted by $\boldsymbol{F}_r$ occurred stress-free in the collagen network while the elastic deformation $\boldsymbol{F}_e$ contributed to the stress response. Conceptually this can be visualised by

the interplay between the free-rotating link element and the spring in the uniaxial model in Fig. 1. With the definition of elastic right Cauchy-Green tensors $\widehat{\boldsymbol{C}}_e = \boldsymbol{F}_e^T \boldsymbol{F}_e$ the energy potential for the anisotropic tissue response was modelled using a continuous angular fibre distribution following a formulation used in [44]

$$\psi_{aniso} = C_4(\boldsymbol{a}_0)\,[I_{4\,e} - 1]^{\beta(\boldsymbol{a}_0)} \quad \text{with} \quad I_{4\,e} \geq 1 \quad \text{and} \quad \beta(\boldsymbol{a}_0) \geq 2 \tag{5}$$

with the anisotropic material parameters $C_4(\boldsymbol{a}_0)$ and $\beta(\boldsymbol{a}_0)$ defining the (strain dependent) stiffness in a fibre direction $\boldsymbol{a}_0$. The modified invariant $I_{4\,e} = \mathrm{tr}\,(\widehat{\boldsymbol{M}}\widehat{\boldsymbol{C}}_e) = \lambda_f^2$ ensured that collagen fibres only contributed stresses once the fibre stretch reached a certain transition value. Here, $\widehat{\boldsymbol{M}}$ is the unit structure tensor of a family of fibres in the remodelled configuration [41].
Collagen network anisotropy was described using an anisotropy tensor

$$\boldsymbol{\Xi} = \sum_{i=1}^{3} \xi_i \boldsymbol{w}_i \otimes \boldsymbol{w}_i \tag{6}$$

with the principal values ξ_i prescribing the degree of structural anisotropy. When the components of the direction vector $\boldsymbol{a}_0$ were expressed in terms of the basis $\{\boldsymbol{w}_i\}$ as $\boldsymbol{a}_0 = \cos\Theta \sin\Phi\, \boldsymbol{w}_1 + \sin\Theta \sin\Phi\, \boldsymbol{w}_2 + \cos\Phi\, \boldsymbol{w}_3$, the material parameter C_4 in a fibre direction were derived via an ellipsoid representation [44] that could be scaled with a parameter m to allow for adjustment of the degree of anisotropy (increasing m leads to a higher degree of ellipticity in the material parameter distribution than given by $\boldsymbol{\Xi}$)

$$C_4(\boldsymbol{a}_0) = \left[\frac{(\cos\Theta \sin\Phi)^2}{\xi_1^{2m}} + \frac{(\sin\Theta \sin\Phi)^2}{\xi_2^{2m}} + \frac{(\cos\Phi)^2}{\xi_3^{2m}}\right]^{-\frac{1}{2}} \frac{\bar{C}_4}{r_m} \tag{7}$$

where $\bar{C}_4$ is a baseline material parameter and $r_m = \frac{1}{3}(\xi_1^m + \xi_2^m + \xi_3^m)$ the mean radius of the ellipsoid. The division by r_m is performed such that in the case of a spherical tensor $\boldsymbol{\Xi}$ one always gets $C_4(\boldsymbol{a}_0) = \bar{C}_4$ irrespective of the magnitude of the scaled eigenvalues $\xi_1^m = \xi_2^m = \xi_3^m$. A numerical processing step ensured constant total fibre network stiffness independent of the degree of ellipticity (i.e. "constant" amount of collagen).

2.2 Fibre reorientation due to remodelling

The collagen network was assumed to remodel its orientation with respect to the local deformation such that the fibre network is reinforced in stretched directions and weakened in compressed directions. Using the spectral decomposition of the right Cauchy-Green tensor

$$\boldsymbol{C} = \sum_{i=1}^{3} \lambda_i^2 \boldsymbol{n}_i \otimes \boldsymbol{n}_i \tag{8}$$

a rotation velocity vector $\boldsymbol{\omega}$ could be derived (for details see [41]) that describes the amount of rotation of the orthonormal basis $\{\boldsymbol{w}_i\}$ of $\boldsymbol{\Xi}$ towards the orthonormal basis $\{\boldsymbol{n}_i\}$ of $\boldsymbol{C}$ proportional

to the angle θ between both systems and depending on a time constant τ_f:

$$\boldsymbol{\omega} = \frac{\theta}{\pi\tau_f}\boldsymbol{e} \tag{9}$$

where $\boldsymbol{e}$ is the rotational axis. With the skew-symmetric tensor $\hat{\boldsymbol{\omega}}$ corresponding to the vector $\boldsymbol{\omega}$, the basis vectors of $\boldsymbol{\Xi}$ were then updated in a time increment Δt using an exponential map algorithm

$$\boldsymbol{w}_i^{n+1} = \exp(\hat{\boldsymbol{\omega}}\Delta t)\boldsymbol{w}_i^n \tag{10}$$

The eigenvalues of $\boldsymbol{\Xi}$ were updated based on the squared principal stretches using a linear rate equation:

$$\dot{\xi}_i = \frac{1}{\tau_f}(\lambda_i^2 - \xi_i) \tag{11}$$

2.3 Remodelling of the stress-free configuration

The stress-free configuration of the collagen network was modelled to evolve based on the assumption that collagen fibres remodel towards a homeostatic stretch value λ_h at which they reside in the matrix. Collagen fibres only contributed to load bearing once stretched above their recruitment stretch λ_r. Corresponding to the uniaxial analogy in Fig. 1, in three dimensions the corresponding geometric information was included into the definition of the remodelling part of the deformation gradient

$$\boldsymbol{F}_r = \sum_{i=1}^{3} \lambda_r(\boldsymbol{w}_i)\boldsymbol{w}_i \otimes \boldsymbol{w}_i \tag{12}$$

Once loading disturbs the homeostatic state of the network and fibres are no longer stretched at their homeostatic value λ_h the recruitment stretch has to change in order to restore tensional network homeostasis. This new desired recruitment stretch λ_0 is related to the applied stretch λ via $\lambda_0 = \lambda/\lambda_h$. The recruitment stretch evolution towards λ_0 was governed by the rate equation

$$\dot{\lambda}_r = \frac{1}{\tau_f}(\lambda_0 - \lambda_r) \tag{13}$$

2.4 ECM synthesis

The accumulation of extracellular matrix (ECM) components such as proteoglycans (PG) and collagen (COL) in cell seeded hydrogels leads to increases in their mechanical properties which changes the stimuli imposed by the bioreactor. Since only the basic phenomenological aspects of biomolecule deposition were of interest, a bilinear model of constituent synthesis was assumed: Initially, a constituent is secreted at a constant rate. Once it reaches a designated final concentration ($\bar{m}_\alpha$) that level is maintained constant:

$$\dot{m}_\alpha = \text{const.}\ , \quad 0 \leq m_\alpha < \bar{m}_\alpha \tag{14}$$

$$\dot{m}_\alpha = 0\ , \quad m = \bar{m}_\alpha \tag{15}$$

where m_α is the current mass of constituent α, i.e. PG or COL. Final amounts of PG and COL were chosen to be 8 % w/w and 16 % w/w, respectively. We assumed that PG production levels off after 42 days and that collagen production is 6 times slower. This is in line with experimental observations showing that after 42 days in culture COL content reaches only a fraction of native values whereas PG build up more quickly [35, 36]. In accordance with the study objective and experimental observations [34, 35, 36], synthesis rates were modelled independent of mechanical stimuli. Therefore, differences in the predicted mechanical properties of dynamically compressed and free swelling constructs in these simulations are purely due to changes in collagen orientation and configuration due to loading.

It was assumed that the material properties of the isotropic ground phase C_1, D_2 remained at agarose values. The fixed charge density c_{F0} was directly related to the current proteoglycan content. The anisotropic material parameter $\bar{C}_4$ was related to collagen content. This is in general agreement with studies that relate tissue composition to mechanical properties [1, 45, 46, 2, 3]. For simplicity, we assumed a simple linear connection between the material parameters and the constituent levels:

$$c_{F0} = c_{F0}(Cart)\frac{m_{PG}}{\bar{m}_{PG}} \tag{16}$$

$$\bar{C}_4 = \bar{C}_4(Cart)\frac{m_{COL}}{\bar{m}_{COL}} \tag{17}$$

2.5 Boundary Conditions

In this study boundary conditions were modelled according to the bioreactor culture protocols used in [35] and [36]. Cylindrical cell seeded constructs were either left free swelling for the entire culture period (FS group) or loaded for 3 hours a day in cyclic unconfined compression and left to swell freely during the remaining 21 hours (DL group).

For remodelling studies the current tissue deformation is of interest. Free swelling could be modelled as an equilibrium load step ($p = 0$). However, it is impractical due to computational limitations to model 3 hours of cyclic loading at 1 Hz (10800 cycles) of a highly nonlinear material. Therefore two simplifying model assumptions were compared:

1. Based on the behaviour of cyclically loaded biphasic materials relaxing to a mean deformation state (see online supplementary material, part A) and the assumption that characteristic time scales at which remodelling occurs are long compared to 1 s ("biological inertia", see online supplementary material, part B) cyclic loading was modelled as an equilibrium load step to the mean level of compression (10 %).

2. Since remodelling could alternatively be directed towards the maximum deformation during a cycle the equilibrium step was followed by a quasi-incompressible compression by the dynamic amplitude (additional 5 %). Incompressibility could be assumed due to the high loading rate (see online supplementary material, part C).

2.6 Evaluated quantities

Construct properties were evaluated in terms of the nominal equilibrium modulus E_{nom} and the apparent equilibrium Poisson's ratio ν_{app}. Additionally, the FS geometry was evaluated in terms of volume and aspect ratio (defined as the ratio of lateral to axial strain in the FS state with respect to the reference geometry prior to swelling). The direction dependent recruitment stretch λ_r and collagen fibre reinforcement ξ were plotted as well.

2.7 Performed simulations

The performed simulations are listed in table 1. Both free swelling (FS) and dynamically loaded (DL) experiments were simulated. Unless otherwise stated in table 1, loading was applied for 3 hours per day. Remodelling either took place with respect to the mean deformation (DL) or the maximum deformation (DL max) during compression.
In "configuration only" simulations, only the recruitment stretch was remodelled and an isotropic fibre stiffness assumed ($\boldsymbol{\Xi} = \boldsymbol{I}$). The value of the homeostatic strain ϵ_h was subjected to a parameter variation.
In "orientation only" simulations, the recruitment stretch was kept unchanged ($\boldsymbol{F}_r = \boldsymbol{I}$) while the fibre stiffness representing orientational effects was allowed to remodel. Since varying m does not produce additional qualitative insight, only one representative simulation was performed.
The "combination" simulations finally combined both effects. This group was used to study the effect of extending the duration of dynamic compression to 6 and 9 hours per day with the $m = 50$ & $\epsilon_h = 2\,\%$ parameter set. To study the relative effects of m and ϵ_h, m was decreased to 10 in a second set of simulations. The parameter values used for all simulations are listed in table 2.
Unless otherwise stated, predicted values at day 56 are provided in the results section. Since both loading and geometry were axisymmetric, the material homogeneous and the model deterministic, constructs remained homogeneous throughout culture. Hence, presented results are representative of any point in the construct geometry.

3 Results

3.1 Fibre distribution

Remodelling of the fibre orientation was predicted to lead to anisotropy in loaded samples whereas free swelling samples were predicted to remain isotropic (Fig. 2). Simulations where only fibre reorientation was considered (Fig. 2a) showed a slightly more anisotropic tissue when remodelling towards the maximum deformation during dynamic loading (DL max) than when remodelling to the mean configuration (DL). Maximum stiffness values were observed in the radial (and circumferential) direction (0° to horizontal) due to fibre reorientation in this direction, whereas the lowest fibre

Table 1: Performed simulations

remodelled feature	parameters	simulations
configuration	$\epsilon_h = 1.5\,\%$	FS, 3 h DL, 3 h DL (max)
	$\epsilon_h = 2\,\%$	FS, 3 h DL, 3 h DL (max)
	$\epsilon_h = 3\,\%$	FS, 3 h DL, 3 h DL (max)
orientation	$m = 50$	FS, 3 h DL, 3 h DL (max)
combination	$m = 50$ & $\epsilon_h = 2.0\,\%$	FS, 3 h DL, 6 h DL, 9 h DL
	$m = 10$ & $\epsilon_h = 2.0\,\%$	FS, 3 h DL

Table 2: Material parameters.

	agarose	cartilage
C_1 [MPa]	$4.34 \cdot 10^{-3}$	$4.34 \cdot 10^{-3}$
ν [-]	0.1	0.1
ϕ_{F0} [-]	0.98	0.8
$\bar{C}_4$ [MPa]	0.0	2.0
$\bar{\beta}$ [-]	2.5	2.5
c_{F0} [meq mm^{-3}]	0.0	0.0002
k [m^4 (N s)$^{-1}$]	$6.61 \cdot 10^{-13}$	$7.5 \cdot 10^{-15}$
c_{ext} [mmol mm^{-3}]	0.00015	0.00015
T [K]	298	298
τ_f [d]	2	2

stiffness was predicted in the axial direction (90° to horizontal).
This trend was maintained in the simulation where realignment was combined with reconfiguration (Figs. 2b and 2c). Increasing the time of dynamic loading from 3 to 6 and 9 hours further increased the anisotropy of the tissue. When the scaling parameter m was decreased from 50 to 10, the collagen architecture itself was predicted to be more anisotropic (Fig. 2c).

3.2 Recruitment stretch distribution

The recruitment stretch distribution remained isotropic in the free swelling samples with anisotropy developing in the loaded samples (Figs. 3a to 3e). The transition stretch with respect to the reference configuration was predicted to increase in the horizontal (radial and circumferential) direction in loaded samples, while it was predicted to decrease in the axial direction. The anisotropy was slightly more pronounced when remodelling was driven by the maximum compressed deformation. The parameter variation of ϵ_h yielded lower recruitment stretch values for higher values of ϵ_h as well as a slightly decreasing degree of anisotropy (Figs. 3a to 3c). In the combined simulations (where both reorientation and reconfiguration occurred), the recruitment stretch distribution was less anisotropic with generally lower values for longer compression times (Fig. 3d).

3.3 Sample Geometry

A higher recruitment stretch in the horizontal direction will lead to preferred swelling into that direction, since fibres start to inhibit deformation at a later stage. A higher fibre stiffness in the horizontal direction however will lead to more swelling into the vertical direction. Hence, in the reconfiguration only simulations, samples with an aspect ratio of $\epsilon_r^0/\epsilon_z^0 \geq 1$, i.e. lower and wider samples, were predicted (Figs. 4a to 4c). In the reorientation only simulations however, the opposite trend, i.e. a higher and more slender sample was predicted (Fig. 4d). For all simulation cases, the free swelling samples remained isotropic and hence maintained an aspect ratio of 1 (Figs. 4a to 4d). With increasing homeostatic strain ϵ_h the FS volume of the samples decreased significantly from $\approx 66\,\mathrm{mm}^3$ for $\epsilon_h = 1.5\,\%$ to $\approx 39\,\mathrm{mm}^3$ for $\epsilon_h = 3.0\,\%$.
In the combined simulations, fibre reorientation led to a decreasing aspect ratio when the scaling parameter m was high (Fig. 7e) but increasing aspect ratios were predicted when a lower value of $m = 10$ was chosen (Fig. 4f). In both cases reconfiguration led to decreasing free swelling volumes in the loaded samples (Figs. 7e and 7f). When loading was simulated for 9 h a day, the FS volume increased again compared to the sample loaded for 6 h. During the initial 14 days of culture, sample volumes and heights were predicted to decrease followed by an increase during the remaining culture period (Fig. 8b).

3.4 Young's Moduli

Strain dependent Young's moduli predictions exhibited stress softening effects (Figs. 5a to 5d). Reconfiguration lead to a stiffness increase in the loaded samples with little difference between

remodelling to the maximum or mean deformation (Figs. 5a to 5c). The magnitude of homeostatic network strain ϵ_h furthermore has a pronounced effect on overall sample stiffness, covering a stiffness range at 10 % strain from ≈ 0.4 to ≈ 1.4 MPa when increasing ϵ_h from 1.5 to 3 %. This was due to the increased amount of pre-strain in the fibre network as well as the associated sample compaction (compare sample volumes in Figs. 4a to 4c). Reorientation on the other hand led to less fibres pre-strained in the loading direction and hence initially softer samples when the constructs were loaded (Fig. 5d).

Combining realignment and reconfiguration caused combined effects. Loaded samples appeared softer than free swelling samples initially but were predicted to have higher stiffnesses with increasing deformation (Figs. 7a and 7b). This effect was more pronounced when loading for 6 h instead of 3 h. However, increasing the time of loading even further did not translate into increased mechanical properties but decreased construct stiffness again (Fig. 5e).

For the combined simulation with $m = 50$ and $\epsilon_h = 2\,\%$ the transient construct development was evaluated at days 0, 12, 28 and 56 in terms of Young's moduli of the FS and DL3 samples (Fig. 8a). Loaded samples were predicted to be stiffer at all time points. The moduli increased monotonically until day 42. Despite an increasing collagen content after day 42, construct properties at day 56 were lower due to the ongoing remodelling of the collagen network than at day 42 (Fig. 8a).

3.5 Poisson's ratios

Poisson's ratio were only marginally influenced by dynamic loading in the reconfiguration only simulations (Figs. 6a to 6c). Fibre realignment, however, led to significant decreases in the Poisson's ratios due to dynamic loading (Fig. 6d). The orientational effect was even more pronounced in the combined simulations with an increasing time of loading leading to decreasing Poisson's ratios and less pronounced nonlinear behaviour (Fig. 6e). For a lower value of m the decrease in Poisson's ratio was less pronounced but generally similar to the $m = 50$ simulation (Fig. 6f).

4 Discussion

In this study we used a computational model based on previous work [41] to investigate changes in the mechanical properties of cell seeded agarose constructs in bioreactor culture from a structural perspective. To the best of our knowledge, this study represents the first theoretical investigation of mechanically induced changes in the orientation and stress-free configuration of the collagen network in a swelling hydrogel during bioreactor culture, and furthermore demonstrates for the first time how alterations to this network can lead to improvements in the mechanical functionality of engineered cartilage tissue. We hypothesised that remodelling of the collagen architecture of tissue engineered constructs in response to dynamic compression can lead to enhanced bulk mechanical properties in the absence of alterations to the biochemical composition, as reported experimentally [34, 35, 36, 38, 37]. Traditionally, collagen fibre orientation is the main architectural feature considered. Fibre reorientation in response to loading, however, caused decreases in bulk construct compressive

stiffness due to the charged nature of the material [43]. The present model additionally considered the local natural configuration of the collagen network. The model predicted that collagen network reconfiguration leads to increased equilibrium moduli while reorientation leads to lowered Poisson's ratios. The model further predicted that the FS geometry of loaded and unloaded samples differs depending on the dominant remodelling mechanism involved. Only when both conformational and orientational changes were considered, could the trends in Young's modulus, Poisson's ratio and sample geometry be predicted simultaneously.

Changes to the collagen's natural configuration were predicted to impact tissue properties by altering the volumetric compaction of the developing tissue and the state of pre-strain in the collagen network. During loading the constructs occupy less volume than in their FS state due to the exudation of fluid. Collagen fibres are laid down and / or remodelled in this configuration. Therefore, for a given homeostatic strain value, the DL samples are compacted to a smaller volume in their unloaded states and hence appeared stiffer due to higher swelling pressures [43]. A lower volume in DL constructs ($52.9\,\mathrm{mm}^3$) compared to FS samples ($53.1\,\mathrm{mm}^3$) at day 42 has been observed experimentally [40]. In addition to altering the volumetric compaction, remodelling the natural configuration also caused changes in the stress softening phenomena associated with the tension-compression nonlinearity [47, 44, 43], with higher collagen network pre-strains predicted to increase the apparent mechanical properties of the construct at equilibrium. Additionally, altering the stress-free state of the collagen network due to loading was predicted to lead to increased aspect ratios, i.e. increased sample radii and decreased heights. Corresponding results have also been reported experimentally [40] where flattening and widening of the samples were observed with a height to radius ratio of 1.02 and 0.91 for FS and DL samples, respectively. Dynamically loaded samples that were up to 20 % thinner in the loading direction than free swelling controls has also been reported [34].

That collagen is incorporated into cartilage ECM under pre-stretch with respect to the free swelling configuration can be demonstrated by digesting the collagen in a cartilage plug and observing its subsequent re-swelling (e.g. [48, 49]). The actual value of ϵ_h is speculative and the natural configurations can only be approximated using inverse simulations. The parameter variation of ϵ_h showed that increasing its value will have a significant effect on construct stiffness.

Experimental evidence is also available for reorientation of the collagen network within engineered cartilaginous constructs in response to extrinsic mechanical signals. For example, no preferred collagen angle has been found using polarised light microscopy in free swelling tissue engineered cartilage while a maximum intensity perpendicular to the loading axis indicates horizontal fibre alignment in dynamically compressed samples [40]. The model also predicted an isotropic fibre architecture in free swelling samples while the maximum value of the anisotropy tensor $\boldsymbol{\Xi}$ was predicted in the horizontal direction within the loaded samples. The apparent Poisson's ratio of engineered cartilaginous constructs has been shown to be lower for loaded (≈ 0.17) than for free swelling (≈ 0.23) samples [40]. Reorientation of the collagen network was predicted to result in

similar changes to the Poisson's ratio of dynamically compressed constructs. Horizontal fibres are more efficient at resisting lateral expansion, which explains the decreases in the Poisson's ratio of the loaded samples. In contrast, the experimentally observed increases in the equilibrium moduli could not be explained by fibre reorientation. Fibre reorientation alone was predicted to lead to higher constructs with a smaller diameter, not consistent with experimental observations [34, 40]. Therefore while fibre reorientation can potentially explain certain experimentally observed phenomena during bioreactor culture such as decreasing Poisson's ratio, it alone cannot explain the effect of dynamic compression on the structural development of engineered cartilaginous constructs.

When combining collagen network realignment and recruitment stretch reconfiguration, a combination of the individual results was predicted. While lower construct properties in the loaded samples were predicted in the initial small strain range, loading led to increased equilibrium properties at higher strains ($\approx$ 5 % strain and higher). A lower Poisson's ratio was also predicted. Thus, combining reorientation and reconfiguration allowed the simultaneous prediction of increased Young's moduli and decreased Poisson's ratios as well as geometrical changes. The interaction of the various constituents was predicted to lead to initial decreases in construct thickness and volume during the initial 14 days of culture followed by an increase thereafter. Initial decreases in sample thickness with subsequent thickening have also been reported experimentally [34]. Our model also predicted a slight increase in equilibrium modulus for 6 h of dynamic compression compared to 3 h (at 10 % applied strain). However, for 9 h of loading the modulus was predicted to decrease again to the level reached after 3 h of loading. This should be seen as a qualitative result. The exact duration of dynamic compression that will produce the stiffest constructs will depend on the parameter values chosen, which are yet to be identified, and other biological effects. Experimentally, no increase in the Young's modulus of engineered constructs has been observed for increasing the daily duration of dynamic compression from 3 to 6 hours [50].

In addition to the daily duration of applied dynamic compression, the total duration of culture will also determine construct mechanical properties. For example, a levelling off of GAG accumulation has been reported for the last two weeks of an 8 week study, while the collagen content continued to increase [34]. Despite that, stiffness values plateaued or even decreased [34]. Our model similarly predicted that after day 42 construct mechanical properties decreased despite increasing collagen content. This was due to ongoing remodelling, namely reconfiguration of the collagen fibres slowly releasing any excess tension in the collagen network previously built up due to increasing swelling pressures. This result emphasises the importance of tissue structure and can partially explain the difficulties in obtaining composition-function relationships. The latter are usually obtained relating bulk biochemical content to biomechanical properties and, as the simulations show, can only be an estimate if structural aspects are neglected.

A number of assumptions had to be made in developing this model. To capture the evolution of the material parameters used in the constitutive model they were related to the main ECM constituents: PG and COL. This evolution was described by a simple bilinear relationship capturing

he basic trends observed in bioreactor culture: Faster PG and slower COL production as well as the resulting increase of construct properties over time. If the synthesis (and degradation) of the constituents itself becomes the focus of study, more sophisticated models will be required. The increases in PGs led to increasing construct volumes due to swelling. Because the offset strain associated with the dynamic compression regime is applied with respect to day 0 geometry, this caused the applied tare strain in the model to change over time in culture. In the isotropic case an increase from 10 % to over 20 % (see online supplementary material, part C), paralleling experimental observations [35], was predicted.

Both agarose and cartilage are porous media in which the pore liquid contributes significantly to the material behaviour. Flow-dependent viscoelastic behaviours can be captured with biphasic models [51]. The bioreactor loading regimen used in this study could be conveniently split up into an equilibrium part, where hydraulic fluid pressurisation was negligible, and a short term quasi-instantaneous part, where fluid flow is negligible. This enabled us to use single phasic constitutive models and compare remodelling towards the mean and the maximum deformation. Advantages to this approach include reduced computation times, increased robustness and no mesh refinements towards free draining boundaries. However, the model cannot be used to investigate the fully transient sample behaviour. Based on the equilibration behaviour of cyclically loaded biphasic tissues and the assumption that biological remodelling takes place on a time scale significantly larger than 1 s we were able to simulate a complete day of loading rather than merely one representative loading cycle. Due to the small time step size it would be computationally infeasible to simulate the complete loading protocol of a day in detail for 56 days with a full biphasic model.

Our phenomenological model makes no mechanistic distinction between cell-mediated and non cell-mediated remodelling. Collagen network remodelling has been observed both in the presence and absence of cells [20]. In tissues with a low cellularity, such as articular cartilage, non cell-mediated mechanisms might play an important role. Strain dependent collagen-collagenase interactions have been reported [52] such that fibres perpendicular to the direction of tensile loading become resorbed which ultimately causes alignment. As long as the mechanism of remodelling in cartilaginous constructs has not been resolved experimentally, simulation can potentially provide insight into the consequences of remodelling.

Using a computational approach, we have been able to provide support for the hypothesis that a mechanoregulated collagen architecture can lead to enhanced bulk mechanical properties of tissue engineered constructs due to mechanical loading with the same biochemical composition as free swelling controls. We further showed that reorientation alone, the traditionally considered architectural feature, is insufficient to capture the experimental observations. This does not invalidate or exclude other hypotheses related to the collagen network that could explain the observed phenomena. Alternative mechanisms likely to be involved include collagen cross-linking and the synthesis of other ECM proteins, such as other collagen types [53, 40, 54]. Studies on heart valve tissue engineering [55, 56] have observed that dynamic loading did not enhance or even decreased bulk

collagen content but did lead to increased cross-linking and mechanical properties of the tissue engineered constructs. [54] found low levels of collagen IX and mature collagen cross-linking to be a major contributing factor to poor mechanical properties of in vitro engineered cartilage. This study also demonstrated that physical stimulation, via centrifugal forces, enhances the mechanical properties of tissue engineered cartilage, implicating enhanced levels of collagen IX and collagen cross-linking for the improvements in construct functionality. These studies suggest an important role for cross-linking and its promotion via dynamic loading in engineering living tissue substitutes. In phenomenological constitutive models both increases in cross-linking and bulk collagen content could be captured via elevated material parameters. This will clearly lead to increases in the apparent mechanical properties in the simulations but does not elucidate whether such phenomena are responsible for the increased mechanical properties reported. While increased properties due to increases in material parameters is an intuitively obvious result, changes in configurational parameters such as fibre orientation and stress-free configuration might be less transparent especially in charged swelling materials and require appropriate models to investigate their possible contribution to the observed changes. Similarly, a number of experimental studies have also shown that dynamic loading can lead to both changes in biochemical composition and mechanical properties [29, 30, 31, 32, 33]. Models such as that presented here might in the future be able to help decouple the relative roles played by compositional and structural changes in determining the mechanical properties of engineered tissues. Another possible mechanism is the altered diffusion of ECM proteins within the samples due to DL. Despite equivalence of the bulk biochemical content DL could lead to different distributions of the ECM proteins and hence affect mechanical properties [53]. However, finite element studies [57] on the local distribution of ECM in tissue engineered cartilage concluded that the global aggregate modulus and permeability were largely insensitive to the microscopic matrix distribution.

While biochemical assays can help determine structure-function relationships, tissue organisation is a determinant of biomechanical functionality in its own right. The effect of organisational alterations is difficult to investigate experimentally, since tissue structure is not easily altered and certain structural features aside from orientation such as natural configurations are difficult to quantify. Uncoupling the relative roles of tissue composition, distribution and organisation at various hierarchical levels is a task amenable to simulation methods. In the future this modelling framework will be extended to other cell types, particularly MSCs, combined with tissue differentiation algorithms and applied to the study of in vivo healing scenarios [18]. For example, a native-like zonal architecture is crucial for successful chondral and osteochondral defect repair. It is for this reason that mechanoregulation algorithms need to include both tissue differentiation and architecture simultaneously in order to understand how environmental factors regulate tissue form and function during skeletal regeneration.

Acknowledgements

We acknowledge funding by IRCSET (G30345) and a Science Foundation Ireland PIYRA award (08/YI5/B1336).

References

[1] Williamson AK, Chen AC, Sah RL. Compressive properties and function-composition relationships of developing bovine articular cartilage. Journal of Orthopaedic Research. 2001;19(6):1113 – 1121. Available from: http://www.sciencedirect.com/science/article/B6W7R-44RNKT6-M/2/deaf1e10cc5d2e42a99305dade682a8a.

[2] Wilson W, Huyghe JM, van Donkelaar CC. Depth-dependent compressive equilibrium properties of articular cartilage explained by its composition. Biomech Model Mechanobiol. 2007 Jan;6(1-2):43–53. Available from: http://dx.doi.org/10.1007/s10237-006-0044-z.

[3] Julkunen P, Jurvelin J, Isaksson H. Contribution of tissue composition and structure to mechanical response of articular cartilage under different loading geometries and strain rates. Biomechanics and Modeling in Mechanobiology. 2009;p. –. Available from: http://dx.doi.org/10.1007/s10237-009-0169-y.

[4] Benninghoff A. Form und Bau der Gelenkknorpel in ihren Beziehungen zur Funktion. Zweiter Teil: Der Aufbau des Gelenkknorpels in seinen Beziehungen zur Funktion. Zeit Zellforsch und Mikroskop Anat. 1925;2:783–862.

[5] Proctor CS, Schmidt MB, Whipple RR, Kelly MA, Mow VC. Material properties of the normal medial bovine meniscus. J Orthop Res. 1989;7(6):771–782. Available from: http://dx.doi.org/10.1002/jor.1100070602.

[6] Taber LA. Biomechanics of Growth, Remodeling, and Morphogenesis. Applied Mechanics Reviews. 1995;48(8):487–545. Available from: http://link.aip.org/link/?AMR/48/487/1.

[7] Taber LA, Humphrey JD. Stress-modulated growth, residual stress, and vascular heterogeneity. J Biomech Eng. 2001 Dec;123(6):528–535.

[8] Gleason RL, Humphrey JD. A mixture model of arterial growth and remodeling in hypertension: altered muscle tone and tissue turnover. J Vasc Res. 2004;41(4):352–363. Available from: http://dx.doi.org/10.1159/000080699.

[9] Hariton I, deBotton G, Gasser TC, Holzapfel GA. Stress-modulated collagen fiber remodeling in a human carotid bifurcation. J Theor Biol. 2007 Oct;248(3):460–470. Available from: http://dx.doi.org/10.1016/j.jtbi.2007.05.037.

[10] Driessen NJB, Bouten CVC, Baaijens FPT. Improved prediction of the collagen fiber architecture in the aortic heart valve. J Biomech Eng. 2005 Apr;127(2):329–336.

[11] Kuhl E, Holzapfel G. A continuum model for remodeling in living structures. Journal of Materials Science. 2007 Nov;42(21):8811–8823. Available from: http://dx.doi.org/10.1007/s10853-007-1917-y.

[12] Grodzinsky AJ, Levenston ME, Jin M, Frank EH. Cartilage tissue remodeling in response to mechanical forces. Annu Rev Biomed Eng. 2000;2:691–713. Available from: http://dx.doi.org/10.1146/annurev.bioeng.2.1.691.

[13] Wilson W, Driessen NJB, van Donkelaar CC, Ito K. Prediction of collagen orientation in articular cartilage by a collagen remodeling algorithm. Osteoarthritis Cartilage. 2006 Nov;14(11):1196–1202. Available from: http://dx.doi.org/10.1016/j.joca.2006.05.006.

[14] Klisch SM, Asanbaeva A, Oungoulian SR, Masuda K, Thonar EJM, Davol A, et al. A cartilage growth mixture model with collagen remodeling: validation protocols. J Biomech Eng. 2008 Jun;130(3):031006. Available from: http://dx.doi.org/10.1115/1.2907754.

[15] van Turnhout M, Kranenbarg S, van Leeuwen J. Contribution of postnatal collagen reorientation to depth-dependent mechanical properties of articular cartilage. Biomechanics and Modeling in Mechanobiology. 2010;p. 1–11. 10.1007/s10237-010-0233-7. Available from: http://dx.doi.org/10.1007/s10237-010-0233-7.

[16] Giori NJ, Beaupr GS, Carter DR. Cellular shape and pressure may mediate mechanical control of tissue composition in tendons. J Orthop Res. 1993 Jul;11(4):581–591. Available from: http://dx.doi.org/10.1002/jor.1100110413.

[17] Cullinane DM, Fredrick A, Eisenberg SR, Pacicca D, Elman MV, Lee C, et al. Induction of a neoarthrosis by precisely controlled motion in an experimental mid-femoral defect. J Orthop Res. 2002 May;20(3):579–586. Available from: http://dx.doi.org/10.1016/S0736-0266(01)00131-0.

[18] Nagel T, Kelly DJ. Mechano-regulation of mesenchymal stem cell differentiation and collagen organisation during skeletal tissue repair. Biomech Model Mechanobiol. 2010 Jun;9(3):359–372. Available from: http://dx.doi.org/10.1007/s10237-009-0182-1.

[19] Humphrey JD. Remodeling of a collagenous tissue at fixed lengths. J Biomech Eng. 1999 Dec;121(6):591–597.

[20] Thomopoulos S, Fomovsky GM, Holmes JW. The development of structural and mechanical anisotropy in fibroblast populated collagen gels. J Biomech Eng. 2005 Oct;127(5):742–750.

[21] Watton PN, Hill NA, Heil M. A mathematical model for the growth of the abdominal aortic aneurysm. Biomech Model Mechanobiol. 2004 Nov;3(2):98–113. Available from: http://dx.doi.org/10.1007/s10237-004-0052-9.

[22] Tomasek JJ, Gabbiani G, Hinz B, Chaponnier C, Brown RA. Myofibroblasts and mechano-regulation of connective tissue remodelling. Nat Rev Mol Cell Biol. 2002 May;3(5):349–363. Available from: http://dx.doi.org/10.1038/nrm809.

[23] Foolen J, van Donkelaar CC, Soekhradj-Soechit S, Ito K. European Society of Biomechanics S.M. Perren Award 2010: An adaptation mechanism for fibrous tissue to sustained shortening. Journal of Biomechanics. 2010;43(16):3168 – 3176. Available from: http://www.sciencedirect.com/science/article/B6T82-50XJC0S-1/2/47b646146d92bb178404711cc88ec093.

[24] Donkelaar CCv, Wilson W. Chondrocyte Hypertrophy Requires Matrix Turnover. In: Proceedings of 2006 Summer Bioengineering Conference, June 21-25, Amelia Island Plantation, Amelia Island, Florida, USA; 2006. .

[25] Temenoff JS, Mikos AG. Review: tissue engineering for regeneration of articular cartilage. Biomaterials. 2000;21(5):431 – 440. Available from: http://www.sciencedirect.com/science/article/B6TWB-3YDGFVB-1/2/3253b30b760e9735db73d4319baac942.

[26] Hunziker EB. Articular cartilage repair: basic science and clinical progress. A review of the current status and prospects. Osteoarthritis and Cartilage. 2002;10(6):432 – 463. Available from: http://www.sciencedirect.com/science/article/B6WP3-461T53D-2/2/7ca22114093bd6a0227fa1b569b90af2.

[27] Koga H, Engebretsen L, Brinchmann J, Muneta T, Sekiya I. Mesenchymal stem cell-based therapy for cartilage repair: a review. Knee Surgery, Sports Traumatology, Arthroscopy. 2009 Nov;17(11):1289–1297. Available from: http://dx.doi.org/10.1007/s00167-009-0782-4.

[28] Iwasa J, Engebretsen L, Shima Y, Ochi M. Clinical application of scaffolds for cartilage tissue engineering. Knee Surgery, Sports Traumatology, Arthroscopy. 2009 Jun;17(6):561–577. Available from: http://dx.doi.org/10.1007/s00167-008-0663-2.

[29] Mauck RL, Soltz MA, Wang CC, Wong DD, Chao PH, Valhmu WB, et al. Functional tissue engineering of articular cartilage through dynamic loading of chondrocyte-seeded agarose gels. J Biomech Eng. 2000 Jun;122(3):252–260.

[30] Buschmann MD, Gluzband YA, Grodzinsky AJ, Hunziker EB. Mechanical compression modulates matrix biosynthesis in chondrocyte/agarose culture. J Cell Sci. 1995 Apr;108 (Pt 4):1497–1508.

[31] Davisson T, Kunig S, Chen A, Sah R, Ratcliffe A. Static and dynamic compression modulate matrix metabolism in tissue engineered cartilage. J Orthop Res. 2002 Jul;20(4):842–848. Available from: http://dx.doi.org/10.1016/S0736-0266(01)00160-7.

[32] Tsuang YH, Lin YS, Chen LT, Cheng CK, Sun JS. Effect of dynamic compression on in vitro chondrocyte metabolism. Int J Artif Organs. 2008 May;31(5):439–449.

[33] Nicodemus GD, Bryant SJ. Mechanical loading regimes affect the anabolic and catabolic activities by chondrocytes encapsulated in PEG hydrogels. Osteoarthritis Cartilage. 2010 Jan;18(1):126–137. Available from: http://dx.doi.org/10.1016/j.joca.2009.08.005.

[34] Mauck RL, Wang CCB, Oswald ES, Ateshian GA, Hung CT. The role of cell seeding density and nutrient supply for articular cartilage tissue engineering with deformational loading. Osteoarthritis and Cartilage. 2003;11(12):879 – 890. Available from: http://www.sciencedirect.com/science/article/B6WP3-49SWBCC-1/2/f33484507367eff3b262cb7434c5fa1d.

[35] Lima EG, Bian L, Ng KW, Mauck RL, Byers BA, Tuan RS, et al. The beneficial effect of delayed compressive loading on tissue-engineered cartilage constructs cultured with TGF-beta3. Osteoarthritis Cartilage. 2007 Sep;15(9):1025–1033. Available from: http://dx.doi.org/10.1016/j.joca.2007.03.008.

[36] Bian L, Fong JV, Lima EG, Stoker AM, Ateshian GA, Cook JL, et al. Dynamic mechanical loading enhances functional properties of tissue-engineered cartilage using mature canine chondrocytes. Tissue Eng Part A. 2010 May;16(5):1781–1790. Available from: http://dx.doi.org/10.1089/ten.TEA.2009.0482.

[37] Hoenig E, Winkler T, Mielke G, Paetzold H, Schuettler D, Goepfert C, et al. High Amplitude Direct Compressive Strain Enhances Mechanical Properties of Scaffold-Free Tissue-Engineered Cartilage. Tissue Engineering Part A. 2011;17(9-10):1401–1411. Available from: http://www.liebertonline.com/doi/abs/10.1089/ten.tea.2010.0395.

[38] Huang A, Farrell M, Kim M, Mauck R. Long-term dynamic loading improves the mechanical properties of chondrogenic mesenchymal stem cell-laden hydrogel. eCells & Materials. 2010;19:72–85.

[39] Mauck RL, Wang CCB, Oswald ES, Ateshian GA, Hung CT. The role of cell seeding density and nutrient supply for articular cartilage tissue engineering with deformational loading. Osteoarthritis Cartilage. 2003 Dec;11(12):879–890.

[40] Kelly TAN, Ng KW, Wang CCB, Ateshian GA, Hung CT. Spatial and temporal development of chondrocyte-seeded agarose constructs in free-swelling and dynamically loaded cultures. Journal of Biomechanics. 2006;39(8):1489 – 1497. Available from: http://www.sciencedirect.com/science/article/B6T82-4GH4B00-1/2/76d2371137ab41375f98c24852d1fd7d.

[41] Nagel T, Kelly D. Remodelling of collagen fibre transition stretch and angular distribution in soft biological tissues and cell-seeded hydrogels. Biomechanics and Modeling in Mechanobiology. 2011;p. 1–15. 10.1007/s10237-011-0313-3. Available from: http://dx.doi.org/10.1007/s10237-011-0313-3.

[42] Görke UJ, Günther H, Nagel T, Wimmer MA. A Large Strain Material Model for Soft Tissues With Functionally Graded Properties. Journal of Biomechanical Engineering. 2010;132(7):074502. Available from: http://link.aip.org/link/?JBY/132/074502/1.

[43] Nagel T, Kelly DJ. The Influence of Fibre Orientation on the Equilibrium Properties of Neutral and Charged Biphasic Tissues. J Biomech Eng. 2010;132(11):114506 (7 pages).

[44] Ateshian GA, Rajan V, Chahine NO, Canal CE, Hung CT. Modeling the Matrix of Articular Cartilage Using a Continuous Fiber Angular Distribution Predicts Many Observed Phenomena. Journal of Biomechanical Engineering. 2009;131(6):061003. Available from: http://link.aip.org/link/?JBY/131/061003/1.

[45] Korhonen RK, Laasanen MS, Töyräs J, Lappalainen R, Helminen HJ, Jurvelin JS. Fibril reinforced poroelastic model predicts specifically mechanical behavior of normal, proteoglycan depleted and collagen degraded articular cartilage. J Biomech. 2003 Sep;36(9):1373–1379.

[46] Ficklin T, Thomas G, Barthel JC, Asanbaeva A, Thonar EJ, Masuda K, et al. Articular cartilage mechanical and biochemical property relations before and after in vitro growth. J Biomech. 2007;40(16):3607–3614. Available from: http://dx.doi.org/10.1016/j.jbiomech.2007.06.005.

[47] Chahine NO, Wang CCB, Hung CT, Ateshian GA. Anisotropic strain-dependent material properties of bovine articular cartilage in the transitional range from tension to compression. J Biomech. 2004 Aug;37(8):1251–1261. Available from: http://dx.doi.org/10.1016/j.jbiomech.2003.12.008.

[48] Maroudas AI. Balance between swelling pressure and collagen tension in normal and degenerate cartilage. Nature. 1976 Apr;260(5554):808–809.

[49] Bank RA, Soudry M, Maroudas A, Mizrahi J, TeKoppele JM. The increased swelling and instantaneous deformation of osteoarthritic cartilage is highly correlated with collagen degradation. Arthritis & Rheumatism. 2000;43(10):2202–2210. Available from: http://dx.doi.org/10.1002/1529-0131(200010)43:10<2202::AID-ANR7>3.0.CO;2-E.

[50] Ng KW, Mauck RL, Wang CCB, Kelly TAN, Ho MMY, Chen FH, et al. Duty Cycle of Deformational Loading Influences the Growth of Engineered Articular Cartilage. Cell Mol Bioeng. 2009 Sep;2(3):386–394. Available from: http://dx.doi.org/10.1007/s12195-009-0070-x.

[51] Mow VC, Kuei SC, Lai WM, Armstrong CG. Biphasic creep and stress relaxation of articular cartilage in compression? Theory and experiments. J Biomech Eng. 1980 Feb;102(1):73–84.

[52] Huang C, Yannas IV. Mechanochemical studies of enzymatic degradation of insoluble collagen fibers. J Biomed Mater Res. 1977;11(1):137–154. Available from: http://dx.doi.org/10.1002/jbm.820110113.

[53] Kelly TAN, Wang CCB, Mauck RL, Ateshian GA, Hung CT. Role of cell-associated matrix in the development of free-swelling and dynamically loaded chondrocyte-seeded agarose gels. Biorheology. 2004 Jan;41(3):223–237. Available from: http://iospress.metapress.com/content/FDYYBTYEWHR0VCGH.

[54] Yan D, Zhou G, Zhou X, Liu W, Zhang WJ, Luo X, et al. The impact of low levels of collagen IX and pyridinoline on the mechanical properties of in vitro engineered cartilage. Biomaterials. 2009;30(5):814 – 821. Available from: http://www.sciencedirect.com/science/article/pii/S0142961208008168.

[55] Balguid A, Rubbens MP, Mol A, Bank RA, Bogers AJJC, van Kats JP, et al. The role of collagen cross-links in biomechanical behavior of human aortic heart valve leaflets–relevance for tissue engineering. Tissue Eng. 2007 Jul;13(7):1501–1511. Available from: http://dx.doi.org/10.1089/ten.2006.0279.

[56] Rubbens MP, Mol A, van Marion MH, Hanemaaijer R, Bank RA, Baaijens FPT, et al. Straining mode-dependent collagen remodeling in engineered cardiovascular tissue. Tissue Eng Part A. 2009 Apr;15(4):841–849. Available from: http://dx.doi.org/10.1089/ten.tea.2008.0185.

[57] Sengers B, van Donkelaar C, Oomens C, Baaijens F. The Local Matrix Distribution and the Functional Development of Tissue Engineered Cartilage, a Finite Element Study. Annals of Biomedical Engineering. 2004;32:1718–1727. 10.1007/s10439-004-7824-3. Available from: http://dx.doi.org/10.1007/s10439-004-7824-3.

Figure legends

Fig. 1: Conceptual visualisation of the recruitment stretch. While the isotropic material (bottom spring; GAGs, agarose) always carry load, the collagen network (top spring) only contributes to the stress response when stretched beyond the recruitment stretch, i.e. when the link element is straitened. The stretches λ, λ_r and λ_f are the one dimensional analogues to the three dimensional deformation gradients $\boldsymbol{F}$, $\boldsymbol{F}_r$ and $\boldsymbol{F}_e$, respectively.

Fig. 2: Direction dependent relative structural anisotropy $\xi(\alpha)/\xi_m$ with $\xi_m = (\xi_1 + \xi_2 + \xi_3)/3$ at day 56. α is the angle to the horizontal (radial) direction. (a) reorientation only simulation; (b) simulation with combined effects. A value greater than on indicates higher than average fibre reinforcement while a value smaller than one indicates a lower than average fibre reinforcement.

Fig. 3: Direction dependent recruitment stretch distribution $\lambda_r(\alpha)$ at day 56. α is the angle to the horizontal (radial) direction.

Fig. 4: Sample volumes and aspect ratios in the free swelling state at day 56. The effect of extending the duration of dynamic compression per day has been studied has been studied in the $m = 50$, $\epsilon_h = 2\,\%$ group (e).

Fig. 5: Young's moduli at day 56. The effect of extending the duration of dynamic compression per day has been studied has been studied in the $m = 50$, $\epsilon_h = 2\,\%$ group (e).

Fig. 6: Poisson's ratios at day 56. The effect of extending the duration of dynamic compression per day has been studied has been studied in the $m = 50$, $\epsilon_h = 2\,\%$ group (e).

Fig. 7: Transient construct development for 0 and 3 hours of loading at various time points in culture. Young's moduli at 10 % strain, collagen and GAG content (a); free swelling volumes and sample thicknesses (b) for the $m = 50$, $\epsilon_h = 2\,\%$ simulations.

Short title for page headings

Remodelling in engineered cartilage.

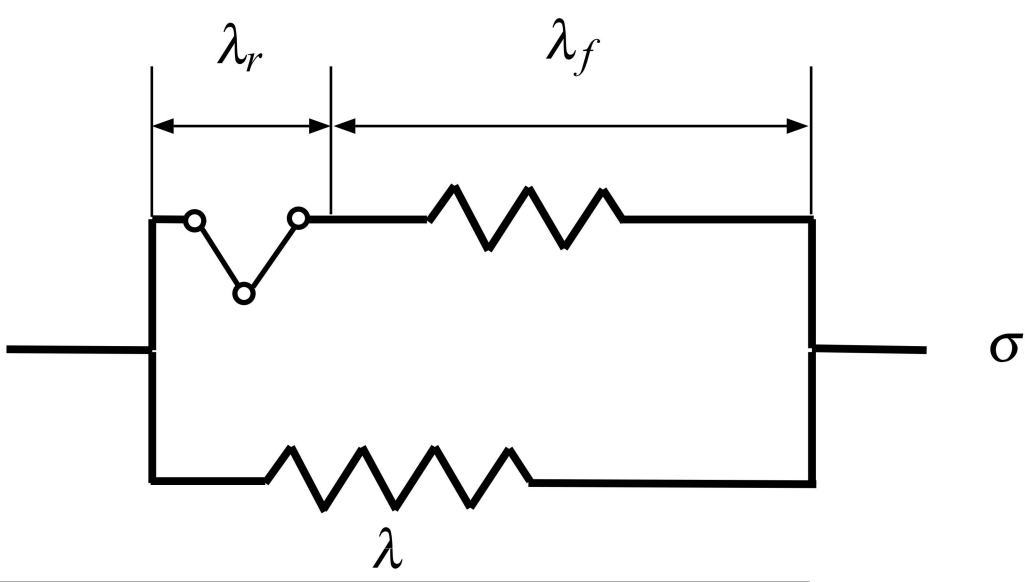
λ_r
λ_f
σ
λ

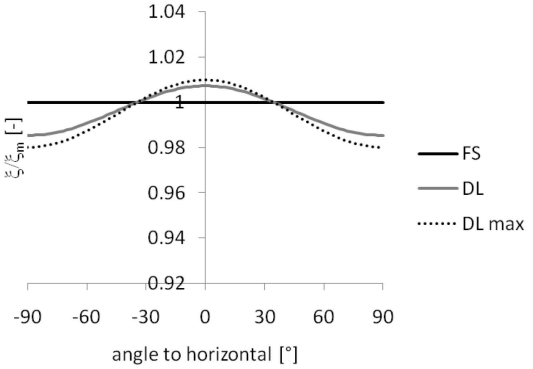

(a) $m = 50$

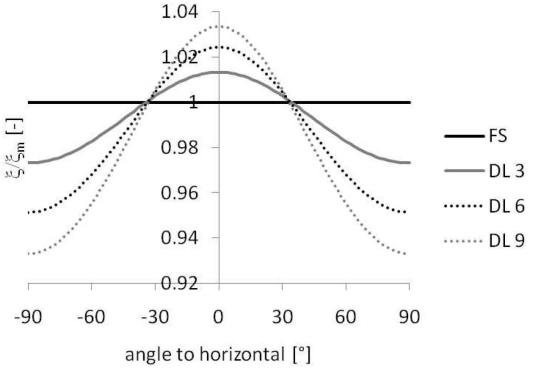

(b) $m = 50.0$ & $\varepsilon_h = 2.0\,\%$

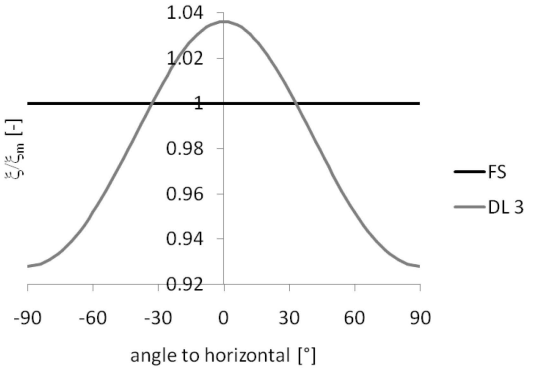

(c) $m = 10.0$ & $\varepsilon_h = 2.0\,\%$

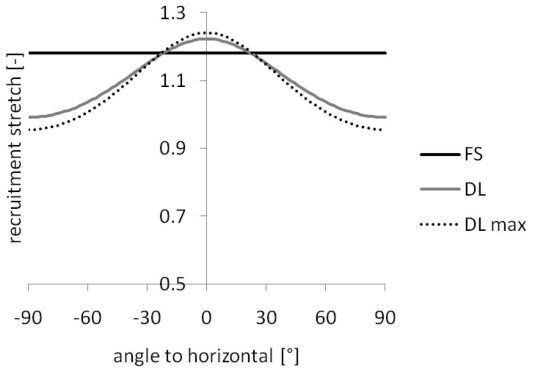

(a) $\varepsilon_h = 1.5\,\%$

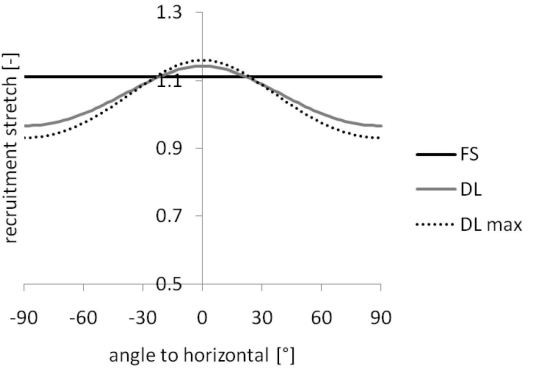

(b) $\varepsilon_h = 2.0\,\%$

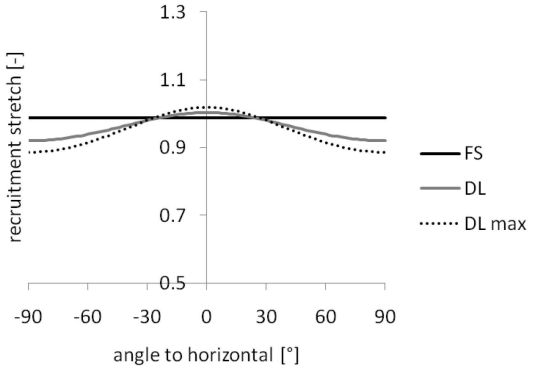

(c) $\varepsilon_h = 3.0\,\%$

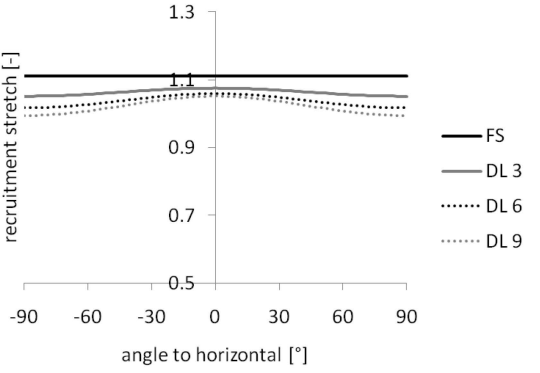

(d) $m = 50.0$ & $\varepsilon_h = 2.0\,\%$

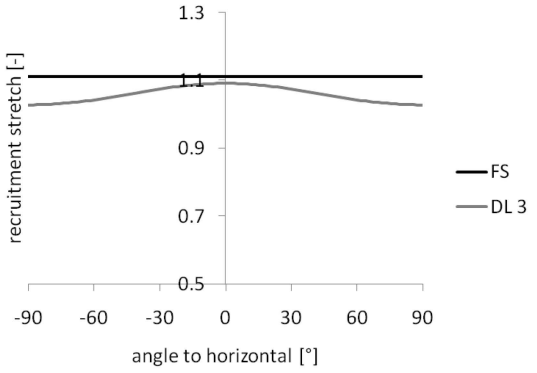

(e) $m = 10.0$ & $\varepsilon_h = 2.0\,\%$

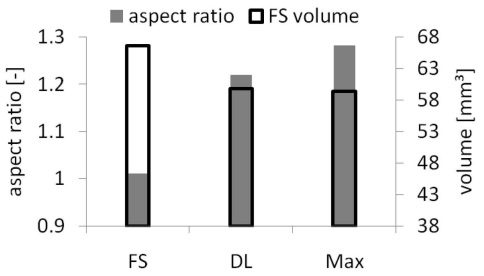

(a) $\varepsilon_h = 1.5\,\%$

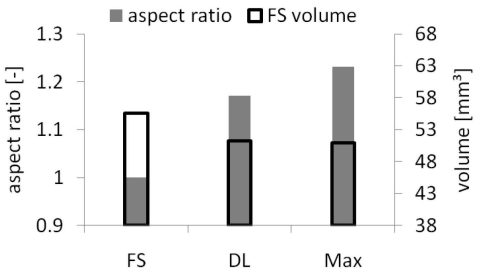

(b) $\varepsilon_h = 2.0\,\%$

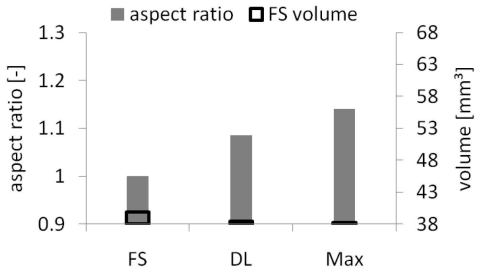

(c) $\varepsilon_h = 3.0\,\%$

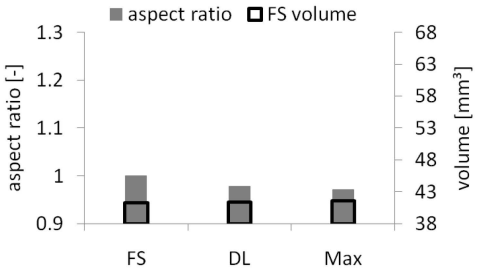

(d) $m = 50.0$

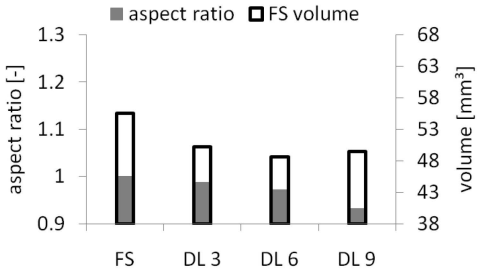

(e) $m = 50$, $\varepsilon_h = 2\,\%$

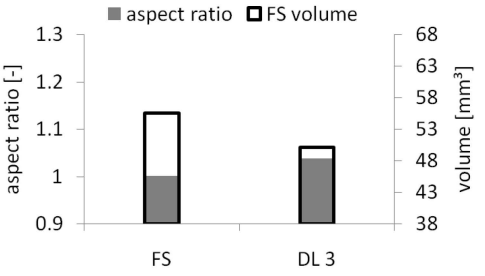

(f) $m = 10$, $\varepsilon_h = 2\,\%$

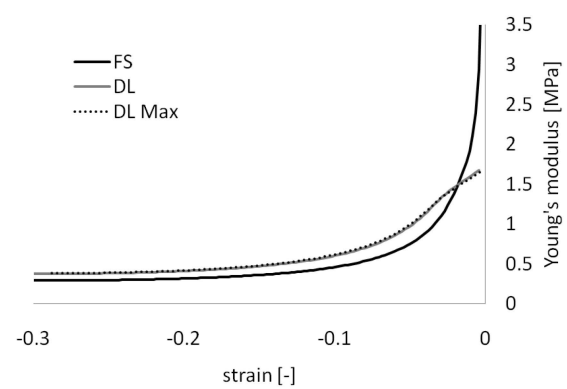

(a) $\varepsilon_h = 1.5\,\%$

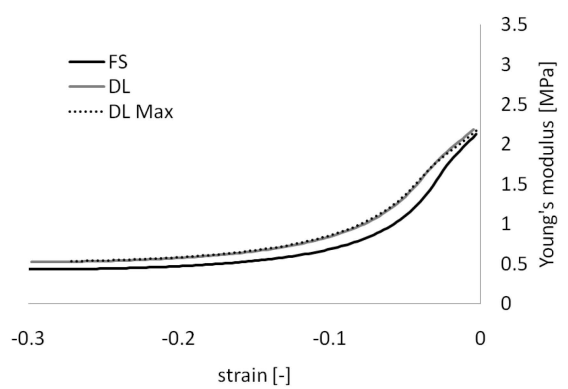

(b) $\varepsilon_h = 2.0\,\%$

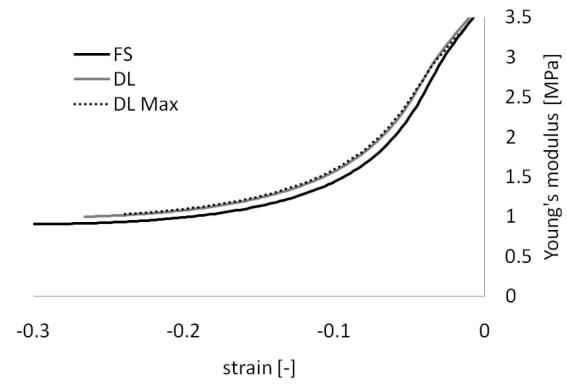

(c) $\varepsilon_h = 3.0\,\%$

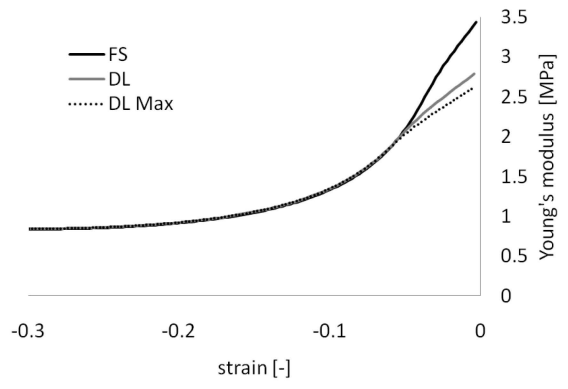

(d) $m = 50.0$

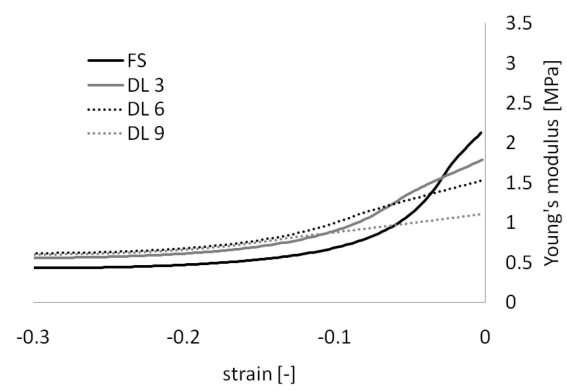

(e) $m = 50$, $\varepsilon_h = 2\,\%$

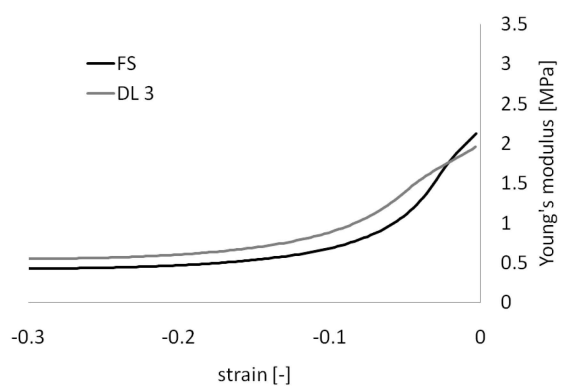

(f) $m = 10$, $\varepsilon_h = 2\,\%$

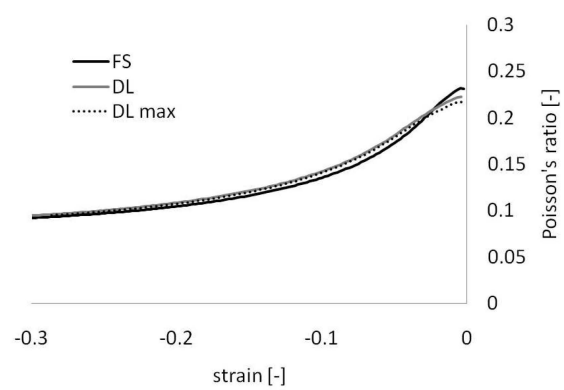

(a) $\varepsilon_h = 1.5\,\%$

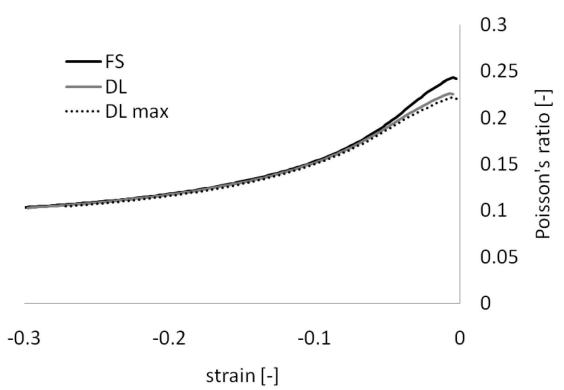

(b) $\varepsilon_h = 2.0\,\%$

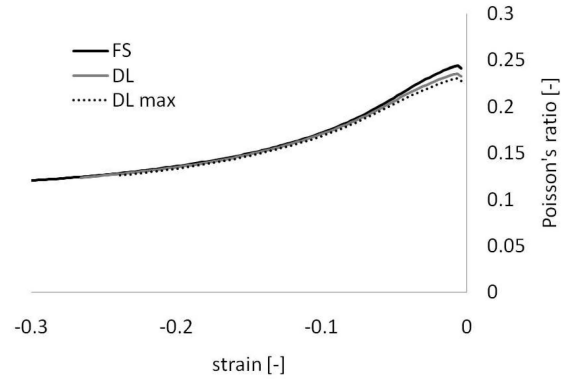

(c) $\varepsilon_h = 3.0\,\%$

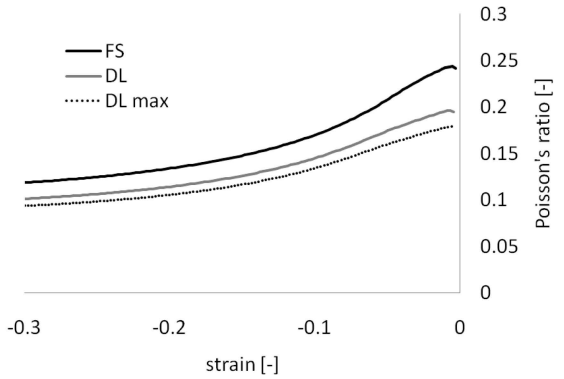

(d) $m = 50.0$

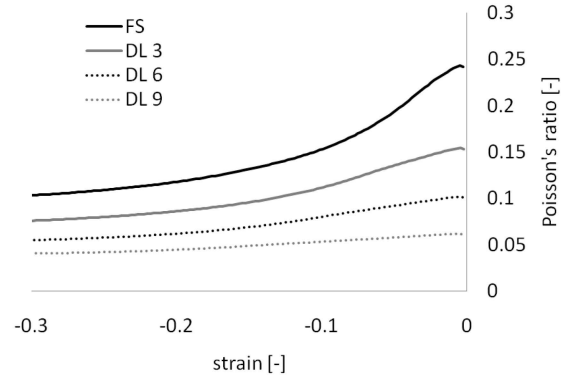

(e) $m = 50$, $\varepsilon_h = 2\,\%$

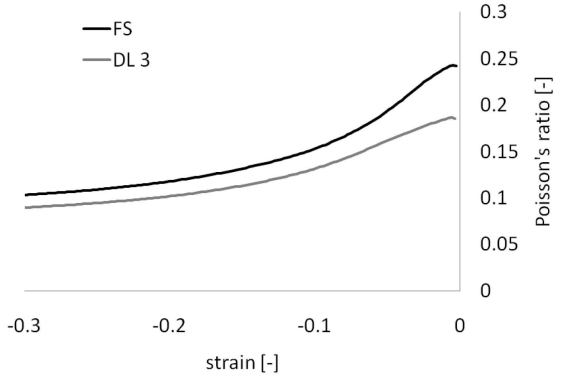

(f) $m = 10$, $\varepsilon_h = 2\,\%$

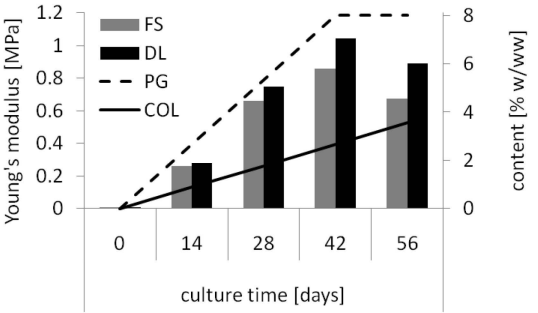

(a) E, COL, GAG

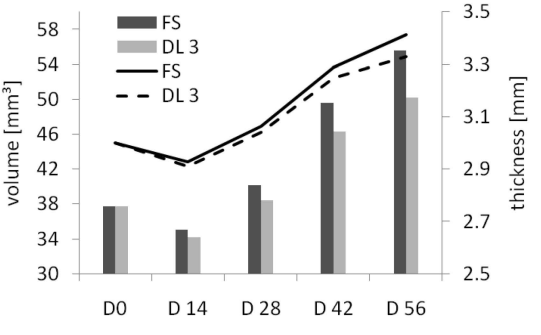

(b) V, t